DOI: 10.11817/j.ysxb.1004.0609.2021-40198

过渡金属磷化物用于电解水析氢反应的研究进展

王 钟[1]，刘家岐[1]，刘 琛[1]，袁 双[1,3,4]，王 强[2]

(1. 东北大学 冶金学院，沈阳 110819；
2. 东北大学 材料电磁过程研究教育部重点实验室，沈阳 110819；
3. 东北大学 低碳钢铁前沿技术研究院，沈阳 110819；
4. 东北大学 辽宁省低碳钢铁技术工程研究中心，沈阳 110819)

摘 要：近年来，随着社会的发展，传统化石能源消耗急剧增加，环境问题日益加剧，可再生清洁能源的开发迫在眉睫。电化学水分解法是公认为将电能转化为氢燃料的一种实用策略。因此，为了实现大规模制氢，开发低成本、资源丰富、高效且稳定的电催化剂至关重要。过渡金属磷化物具有价格低廉、资源丰富、化学稳定性等特点，被广泛应用于电催化析氢领域。本文总结了过渡金属磷化物用于电催化析氢的制备方法，且详细概述了从形貌设计、界面调控、材料复合 3 个方面，提高电解水析氢反应性能，并对其今后发展趋势以及面临的机遇和挑战进行展望。

关键词：过渡金属磷化物；析氢反应；形貌设计；界面调控；材料复合
文章编号：1004-0609(2021)-11-3344-18 **中图分类号**： **文献标志码**：A

引文格式：王 钟, 刘家岐, 刘 琛, 等. 过渡金属磷化物用于电解水析氢反应的研究进展[J]. 中国有色金属学报, 2021, 31(11): 3344−3361. DOI: 10.11817/j.ysxb.1004.0609.2021-40198

WANG Zhong, LIU Jia-qi, LIU Chen, et al. Recent progress of transition metal phosphides in hydrogen evolution reaction of electrolyzed water[J]. The Chinese Journal of Nonferrous Metals, 2021, 31(11): 3344−3361. DOI: 10.11817/j.ysxb.1004.0609.2021-40198

我国虽然能源种类众多，但是化石燃料储量较少。就目前而言，我国煤炭与石油的使用占据能耗总量的 80%以上，且化石燃料中普遍存在氮、硫等元素，这类元素在一定的条件下会和氧发生反应，产生 NO_2、SO_2、SO_3 等酸性气体，对环境造成严重的污染。当遇到水时，这些酸性气体会和水发生反应生成对应的酸，渗进土壤，破环土地的酸碱度，造成农作物大量减产[1−2]。因此，人类开发可再生绿色清洁的能源刻不容缓[3−6]。氢气作为理想燃料，在所有化学燃料中具有最高的质量能量密度，是替代化石燃料清洁能源的最佳载体[7−8]。现阶段制取氢气的 3 种主要方法(如图 1)：电解水制氢、化石能源制氢、生物能制氢[9−11]。其中电解水制氢具有纯度高、成本低、安全且环保等优势，但制氢过程的能耗问题也不可忽略[12]。为了减少供电能耗，提高催化效率，需要更高效的催化剂来制取氢气，以便能在低电位下提供较大的电流密度。目前，贵金属铂是电催化制氢公认的催化材料，但是其价格昂贵且储存量低，刺激了人们对其他高效非贵金属催化材料的探索[13]。当前，对于非贵金属催化材料的研究集中在过渡金属碳化物、过渡金属硫化物、过渡金属氮化物、过渡金属氧化物和过渡金属磷化物(TMPs)[14−18]。很多金属在化反应制取氢气过程中，由于表面与吸附的氢两者间作用太强，从而导致

基金项目：国家自然科学基金青年基金资助项目(21701022)；中国科协青年人才托举工程资助项目(2018QNRC001)；辽宁省兴辽英才计划青年拔尖人才资助项目(XLYC1807214)；中央高校基本科研业务费资助项目(N2124007-1)
收稿日期：2021-05-06；**修订日期**：2021-08-19
通信作者：袁 双，副教授，博士；电话：024-83681171；E-mail：yuans@smm.neu.edu.cn

氢难以脱附，表现出较差的析氢性能。然而，过渡金属中磷元素的存在可以有效地降低吸附氢的自由能，并且 TMPs 能够在更宽的 pH 区间内保持结构稳定，因而 TMPs 成为非贵金属催化剂材料研究热点[19]。

本文对最近年来过渡金属磷化物电解水制取氢气进行综合分析。本文侧重点主要集中在过渡金属磷化物的制备、提高 HER 催化性能的方法以及结构−组成与催化性能之间存在的构效关系。最后，总结了过渡金属磷化物作为析氢反应催化剂所面临的挑战，并且提出了其未来的发展方向。

1　过渡金属磷化物制备方法

过渡金属磷化物可以分为负载型和非负载型，其中单金属磷化物最为常见，但由于双金属之间的协同作用，所以双金属磷化物逐渐成为热门研究材料[20]。由于，过渡金属磷化物中的磷源可以为红磷、白磷、三正辛基膦、三苯基膦、亚磷酸盐、次磷酸盐等[21−24]，所以其制备方法多样化。早期，科研人员深入研究了多种 TMPs 合成方法：元素化合法、固态置换反应法、磷化氢反应法、有机金属分解法、熔融盐电解法等(见表 1)，但该类制备方法需要高温、高压的外界环境，并且原材料价格昂贵,因此限制了他们的实际应用。下面将详细讲述几种常用的 TMPs 制备方法：液相反应法、气固反应法、热解还原法、电沉积法(见表 2)。

液相反应法是在惰性气体保护下，将原材料(过渡金属盐溶液、金属化合物、磷源)充分混合进行化学反应。该化学反应中的磷源通常采用三辛基膦(TOP)、三苯基膦(TPP)、三苯基膦(PPh3)、三辛基氧化膦(TOPO)等有机膦作为磷源，高温下这些化合物中的 C—P 键会发生明显的断裂，从而与金属盐溶液中的金属源发生化学反应[25−27]。TMPs 的尺寸、结构、形貌取决于反应温度、磷化物种类和原材料的配比。由于反应需要有机膦作为磷源及高温条件，所以反应体系易腐蚀、易燃烧，因此，需要在实验过程中持续通入惰性气体。WANG 等[28]采用不同的磷化方式获得了 3 种 Ni_2P/SiO_2 催化剂，当预先还原 Ni/SiO_2 时，即使在 443 K 的温度下，高度分散的纳米镍颗粒也很容易被 PPh3 磷化，结果表明在这种情况下的纳米镍颗粒完全被磷化，最终，合成了细小且均匀的 Ni_2P 纳米颗粒(6 nm)。PAN 等[29]将 TOP 和乙酰丙酮作为磷源和镍源，在油胺溶液中制备了碳纳米管负载的 Ni_2P 纳米颗粒(见图 2(a))，极大提高了比表面积。

气固反应法的磷源以次磷酸钠(NaH_2PO_2)、次磷酸铵($NH_4H_2PO_2$)、红磷(P)为主，当加热温度升高至 250 ℃以上时，次磷酸钠、次磷酸铵便会分解产生磷化氢(PH_3)，对于红磷而言，当加热温度超过 400 ℃时会产生磷蒸汽。在管式炉内，将磷源置于上风处，高温分解后产生的磷化氢或磷蒸汽与下风处的金属源反应生成 TMPs。其中，次磷酸盐热分解法工艺简单，无需高温、高压、程序升温等复杂步骤,因此被公认为最具有前景的 TMPs 制备方法。LI 等[30]通过液相法将 FeO_x 生长在碳纳米管上

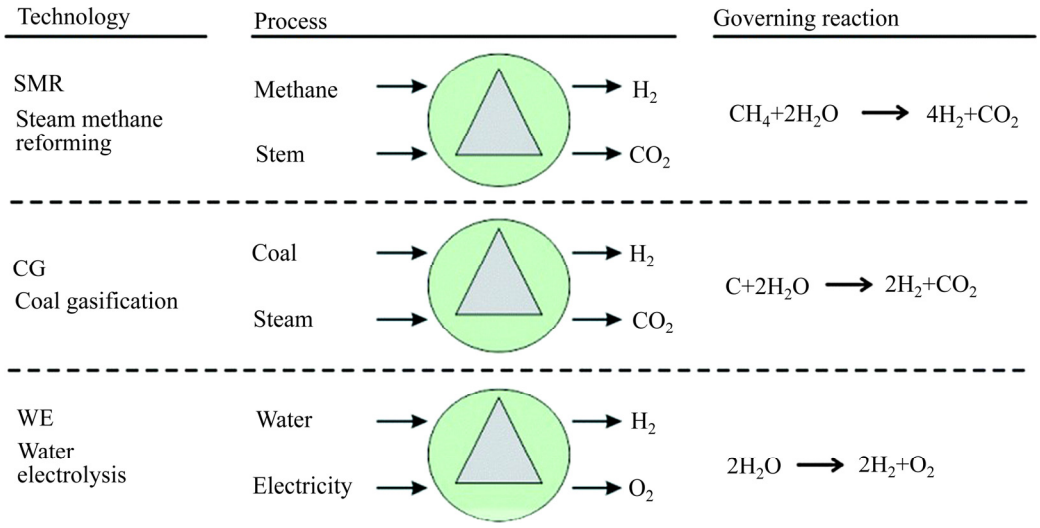

图 1　制取氢气方法示意图[9]

Fig. 1　Schematic diagram of hydrogen production[9]

表 1 早期过渡金属磷化物制备方法

Table 1 Preparation method of early transition metal phosphide

Synthetic method	Reaction principle
Elemental combination method	$M^0+xP^0 \longrightarrow MP_x$
Solid state displacement reaction method	$MCl_x+Na_3P \longrightarrow MP+NaCl$
Phosphine reaction method	$MCl_x+PH_3 \longrightarrow MP+HCl+H_2$
Organic metal decomposition method	$TiCl(PH_2C_6H_{11})_2 \longrightarrow TiP+PH_3+HCl+C_6H_{11}$
Molten salt electrolysis method	$MO_x+H_2 \longrightarrow MP+H_2O$

表 2 常见过渡金属磷化物制备方法概述

Table 2 Overview of preparation methods of common transition metal phosphides

Synthetic method	Advantage	Inferiority
Liquid phase reaction method	Uniform dispersion Controllable morphology	Expensive raw materials Toxic gas generation
Gas solid reaction method	Simple process Without high temperature	High cost Limited production
Pyrolytic reduction method	Large scale production	High temperature and pressure
Electrodeposition method	Relative safety Low synthesis temperature	Uneven deposition Uncontrollable morphology
Hydrothermal method	Low cost Simple operation	Larger size High temperature and pressure

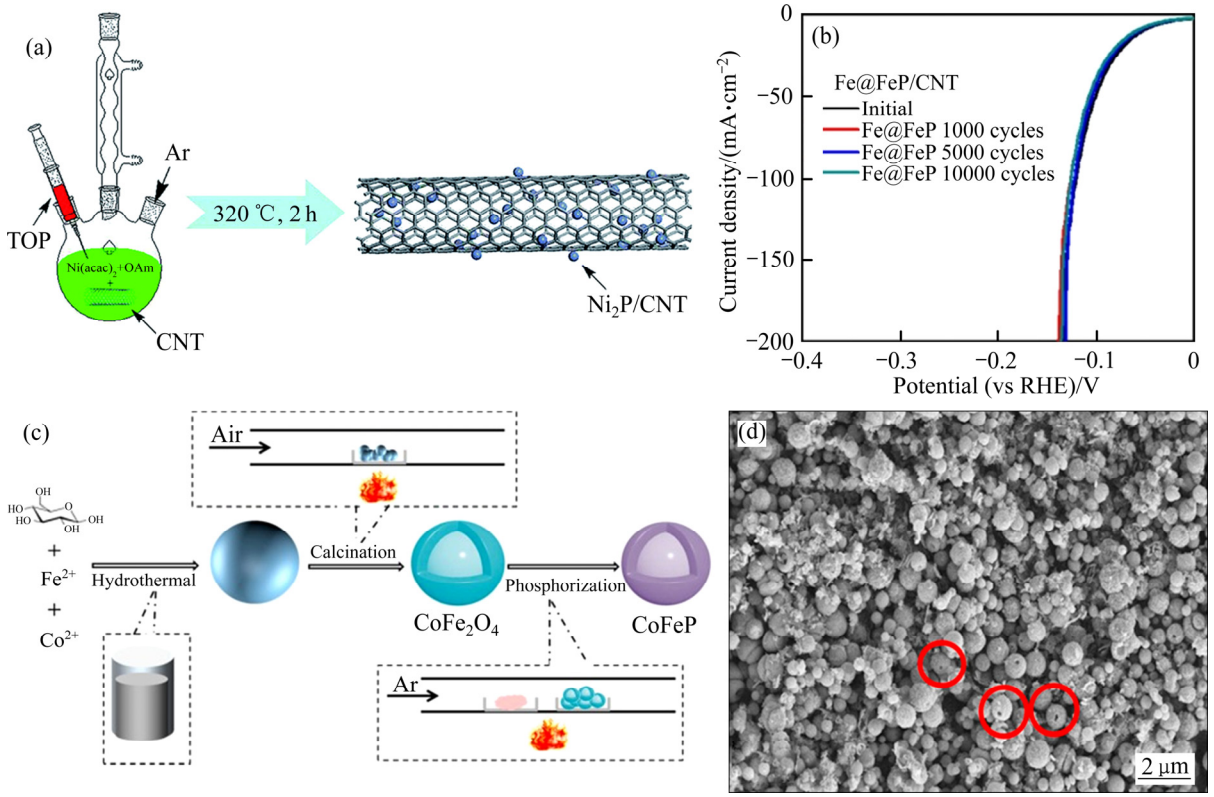

图 2 液相反应法和气固反应法的制备流程图及形貌与性能测试：(a) 液相反应法[29]；(b) Fe@FeP/CNT 稳定性测试[30]；(c) 气固反应法[31]；(d) $CoFe_2O_4$ 空心球结构[31]

Fig. 2 Preparation flow chart, morphology and performance test of liquid phase reaction method and gas solid reaction method: (a) Liquid phase reaction method[29]; (b) Stability test of Fe@FeP/CNT[30]; (c) Gas solid reaction method[31]; (d) Hollow sphere structure of $CoFe_2O_4$[31]

(FeO_x/CNT)，然后在 350 ℃下被氢气还原为 Fe/CNT，接着在氩气保护下与 NaH_2PO_2 磷化，最后，生成了核壳纳米粒子(Fe@FeP/CNT)。作者对该材料做了稳定性测试(见图 2(b))，发现金属与磷化物之间的电子相互作用，可以将氢原子的结合强度提高到最佳水平。图 2(c)展示了一个典型案例[31]，首先葡萄糖分子、钴离子和铁离子在水热条件下反应生成过渡金属氧化物前驱体，其次在空气中煅烧 2 h，得到 $CoFe_2O_4$ 空心球(见图 2(d))，然后将 NaH_2PO_2 和 $CoFe_2O_4$ 空心球分别置于管式炉上游和下游，加热至 400 ℃并保温 2 h，最终成功制备了双金属 CoFeP 空心球。

热解还原法被应用于大规模 TMPs 的制备,该方法多以磷酸盐、亚磷酸盐、多金属氧酸盐、植酸等作为磷源，金属盐作为金属源，在高温(500~1000 ℃)及还原气氛(Ar/H_2)条件下 P—O 键断裂与金属离子结合生成 TMPs。MA 等[32]采用该方法规模化制备了氮掺杂碳壳包覆的纳米晶体(CoMoP@C)，由于碳壳拥有较强的质子吸收能力，因此，极大地提高析氢性能。结果表明，当测试溶液的 PH 范围在 0~1 时，CoMoP@C 的析氢性能接近商业 Pt/C，当 pH 范围在 2~14 时，CoMoP@C 的析氢性能优于商业 Pt/C。LU 等[33]以 MIL-88A 为前驱体，植酸为磷源，合成了镍掺杂 FeP/C 空心纳米棒。WANG 等[34]通过简单的室温搅拌制备了高度均匀的 ZIF-67 纳米立方体(见图 3(a))，然后将植酸溶液加入含有一定量 ZIF-67 和聚乙烯吡咯烷酮(PVP)的乙醇溶液中，在程序升温还原条件下，磷酸基中的 P—O 键被破坏，生成 CoP/C 纳米颗粒(见图 3(b))。

电沉积法的磷源一般采用次磷酸钠，基底可用铜箔、钛箔、碳布、泡沫镍等，反应机理是溶液中金属离子和 $H_2PO_2^-$ 生成 TMPs 吸附在基底表面。该制备方法具有低成本和低能耗的特点，但也存在难以控制 TMPs 的细致结构。CHENG 等[35]探讨了电沉积方式(直流、脉冲)、沉积时间、电流和电压大小对 TMPs 的影响。PEI 等[36]采用一步式恒流密度电沉积法在钛片上沉积了高活性和廉价的 Co-Ni-P 薄层(见图 3(c))。CAO 等[37]以 0.2 mol/L $NiCl_2{\cdot}6H_2O$ 溶液、0.2 mol/L $NaH_2PO_4{\cdot}H_2O$ 溶液、0.25 mol/L NH_4Cl 溶液和 5 种不同含量的 $CuCl_2{\cdot}2H_2O$ 溶液(0 mol/L、0.01 mol/L、0.02 mol/L、0.03 mol/L、0.04 mol/L)制备电解质，并在 10 mA/cm^2 的恒定电流密

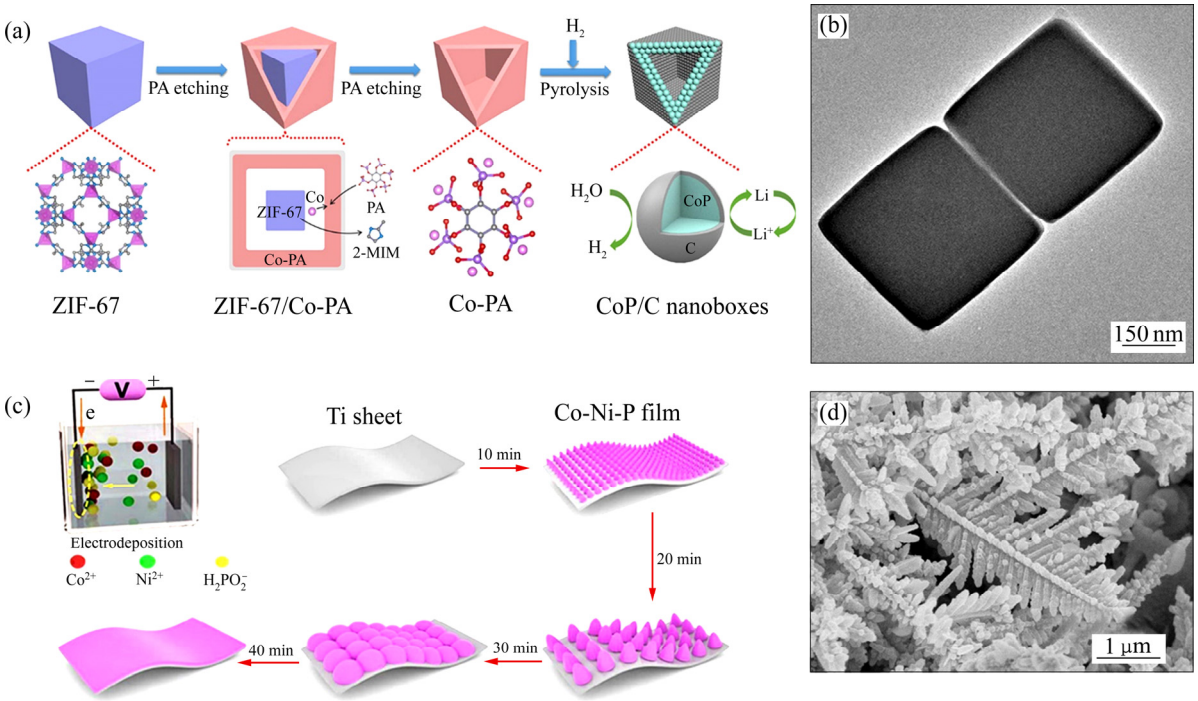

图 3　热解还原法和电沉积法的制备流程图及形貌：(a) 热解还原法[34]；(b) ZIF-67，TEM 像[34]；(c) 电沉积法[36]；(d) Ni-Cu-P，SEM 像[37]

Fig. 3　Preparation process and morphology of pyrolytic reduction method and electrodeposition method: (a) Pyrolysis reduction method[34]; (b) Zif-67, TEM image[34]; (c) Electrodeposition method[36]; (d) Ni-Cu-P, SEM image[37]

度下持续 20 min，发现铜离子的浓度是形成空心树枝状结构(见图 3(d))的关键因素。YANG 等[38]在碳布上电沉积了 Ni-P 纳米颗粒，该颗粒填充 CC 表面上未被 Ni_2P 纳米片占据的位置。实验发现，Ni-P 纳米颗粒的电沉积时间对 Ni-P/Ni_2P/CC 复合材料的催化性能有显着影响，当电沉积的时间较短(60 s)时，可能无法提供足够的活性位点，然而，沉积时间的较长(180 s)时，则可能会导致 Ni_2P 的一些活性位点被覆盖。因此，合适的沉积时间对材料的催化活性尤为重要。

近年来，随着能源结构的调整，吸引大量研究人员探索新的过渡金属磷化物制备方法，例如水热法、溶剂热法、微乳液法、超临界二氧化碳法和室温固相合成法等[39−43]。在众多的方法里，其中溶剂热法和水热法被普遍使用。水热法制备流程为首先使用密闭反应釜作为反应设备，以水溶液或者其他溶剂作为反应介质，然后，在高温高压下进行的反应。该方法与传统方法相比，溶剂热/水热制备流程比较简单，产生的磷化物具有更大的比表面积、更稳定的结构、更多的活性位点[44−46]。

2 过渡金属磷化物析氢性能调控

由于过渡金属磷化物制备方式的多样化，因此，科研人员制备了多种纳米结构。第一类结构包括纳米团簇、纳米线、纳米管、纳米片、纳米阵列等[47−50]，此类结构的合成需要通过粘结剂将活性物质修饰在导电界面上，从而导致活性位点被覆盖，造成堆积现象[51−52]。第二类为自支撑结构，为了避免活性物质集聚，将活性物质直接负载在自支撑电极上如铜箔、钛箔、碳布、泡沫镍等[53−57]。TMPs 形貌结构、导电性以及活性位点是影响 HER 性能的关键因素[58]，因此，本文从形貌设计、界面调控、材料复合三个途径作为研究重点，分析具有独特结构、良好导电性、多活性位点的过渡金属磷化物。

2.1 形貌设计

设计特定结构，可以增加比表面积，从而暴露更多的活性位点[59−62]，因此，优化催化剂纳米结构来构建高效的形貌是实现析氢活性和稳定性的重要因素[63]。CHANG 等[64]用油包水微乳液法制备了单晶镍 $Ni_{12}P_5$ 空心球结构。该材料具有独特的空心结构、较高的比表面积(222.5 m^2/g)以及丰富的孔隙率，从而提供了有效的扩散通道和更多的催化活性中心，增强了催化析氢活性。在酸性溶液中，当电流密为 100 mA/cm^2 时，过电位 277 mV，并且 Tafel 斜率仅为 46 mV/dec(见图 4(a))，与此同时，空心球结构具有良好的稳定性，因此在 12 h 电位测试中，$Ni_{12}P_5$ 空心球催化剂仍能表现出较高活性(见图 4(b))。2018 年，该团队[65]首次在碳纸上制备出了海胆状三元钴磷硫化物(CoPS/CP)，这种独特的海胆状结构有利于电子传导，加速界面反应。在 0.5 mol/L H_2SO_4 溶液中，CoPS/CP 的起始点位为 4 mV，Tafel 斜率为 42.6 mV/dec。通过 DFT 理论计算得知 CoPS/CP 的氢吸附自由能(ΔG_{H^*})为−0.12 eV(见图 4(c))，因此，海胆状结构为高活性且稳定的催化材料提供了选择。类似地，YANG 等[66]通过低温磷化法合成出海胆状的 CoP 纳米晶，该催化剂在酸性溶液中表现出优异的 HER 活性，产生电流密度 100 mA/cm^2 时，过电位 180 mV(见图 4(d))。CHEN 等[67]以三苯基膦为磷源，控制特有的磷化过程，合成了棒状和花状的 Co_2P，该形状具有较大的孔隙率以及比表面积(见图 4(e)~(h))。总而言之，科研人员制备了多种不同的纳米结构，其目的是为了获得更大的比表面积，从而增加该材料活性位点的数量，以此来促进催化剂整体的析氢活性。

研究者发现对 TMPs 空间维度的调控，可以改变电荷分布和诱导局域电场[68−70]。零维(0D)纳米颗粒结合了低密度和高承载能力的特点，因此该维度材料受到了广泛关注。WANG 等[71]提出了在磁场下制备具有可控壳厚度的 0D Co_2P 纳米颗粒(见图 5(a)~(d))，并且讨论了磁场进行壳调谐的机理：磁场可以通过加速溶解过程并减慢柯肯德尔效应过程来减小粒径、调节壳的厚度。这项工作为尺寸可调的过渡金属磷化物空心颗粒的合成提供了一种合理的方法。一维(1D)纳米材料具有高效电子传输能力，被广泛应用于析氢反应。LIN 等[72]采用简单原位磷化法,在不同温度下合成了 1D 多孔的 CoMoP 纳米管(见图 5(e))，结果表明，磷化温度 600 ℃时 CoMoP 纳米管展现出最佳催化性能，在 0.5 mol/L H_2SO_4 溶液中，当电流密度达 10 mA/cm^2 时，过电位为 220 mV，Tafel 斜率为 136 mV/dec。两维(2D)材料有较大的比表面积，这将有利于活性物质与电解液之间发生反应。TANG 等[73]报道了电

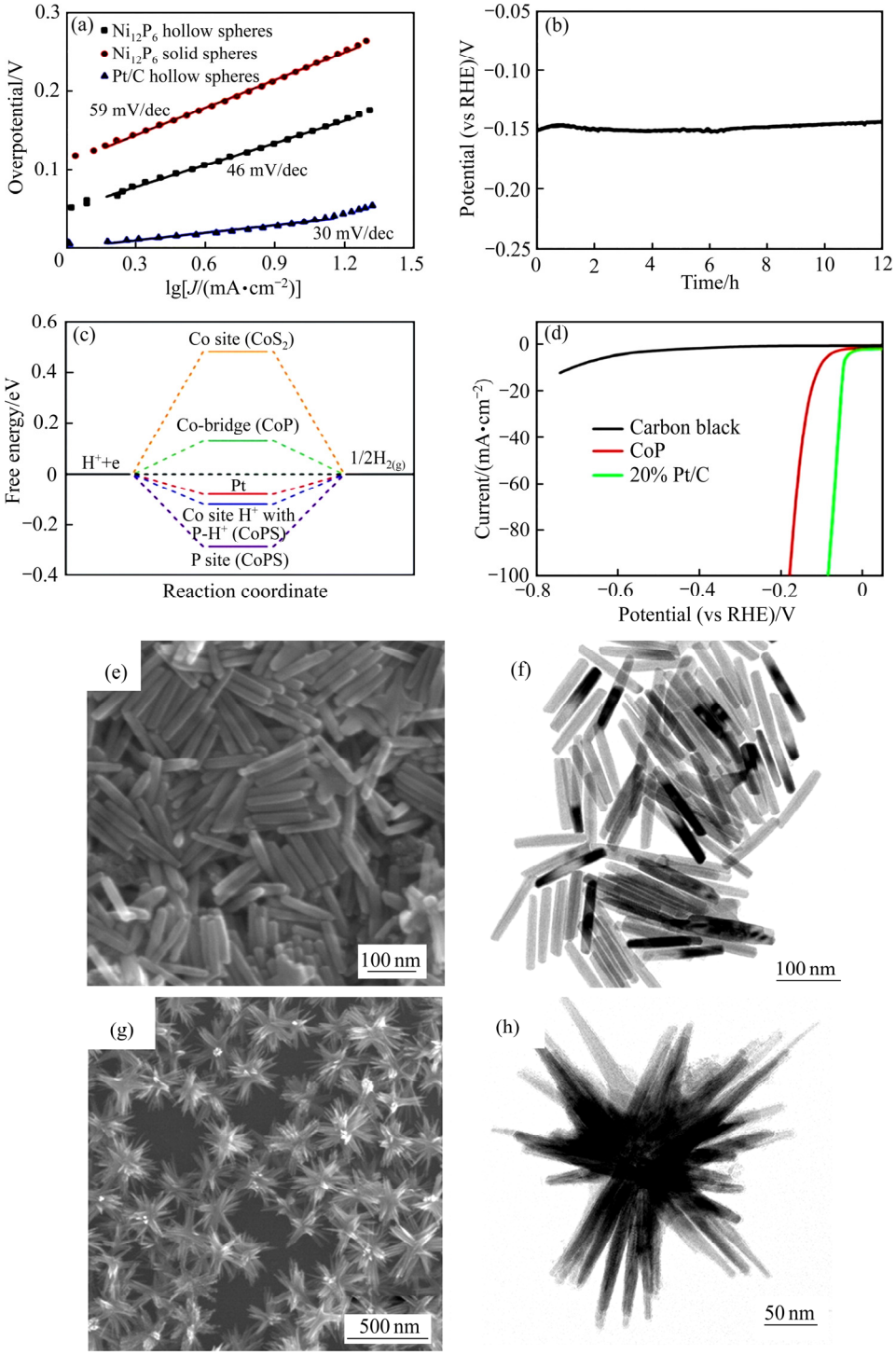

图 4　特定空间结构的纳米材料形貌及催化性能：(a) $Ni_{12}P_5$ 空心球结构、$Ni_{12}P_5$ 实心球结构及 Pt/C 的塔菲尔曲线[64]；(b) 电流密度为 10 mA/cm^2 经过 12 h 时 $Ni_{12}P_5$ 空心球结构的电位−时间曲线[64]；(c) 电压 U=0 V、pH=0 时相对于标准氢电极所计算出 CoPS/CP 的自由能[65]；(d) 炭黑、CoP 以及 Pt/C 在 0.5 mol/L H_2SO_4 中扫速为 5 mV/s 时的极化曲线[66]；(e) Co_2P 纳米棒的扫描电镜图[67]；(f) Co_2P 纳米棒的扫描透射电镜图[67]；(g) Co_2P 纳米花的扫描电镜图[67]；(h) Co_2P 纳米花的扫描透射电镜图[67]

Fig. 4　Morphology and catalytic properties of nano materials with specific spatial structure: (a) Tafel plots of $Ni_{12}P_5$ hollow spheres, $Ni_{12}P_5$ solid spheres and Pt/C[64]; (b) Potential time curve of $Ni_{12}P_5$ hollow sphere structure with current density of 10 mA / cm^2 after 12 h [64]; (c) Calculated free energy of CoPS/CP related to that of standard hydrogen electrode at voltage U=0 V and pH=0[65]; (d) Polarization curves of carbon black, cop and Pt/C in 0.5 mol/L H_2SO_4 at 5 mV/s[66]; (e) SEM image, Co_2P nanorods[67]; (f) TEM image, Co_2P nanorods[67]; (g) SEM image, Co_2P nanoflowers[67]; (h) SEM image, Co_2P nanoflowers[67]

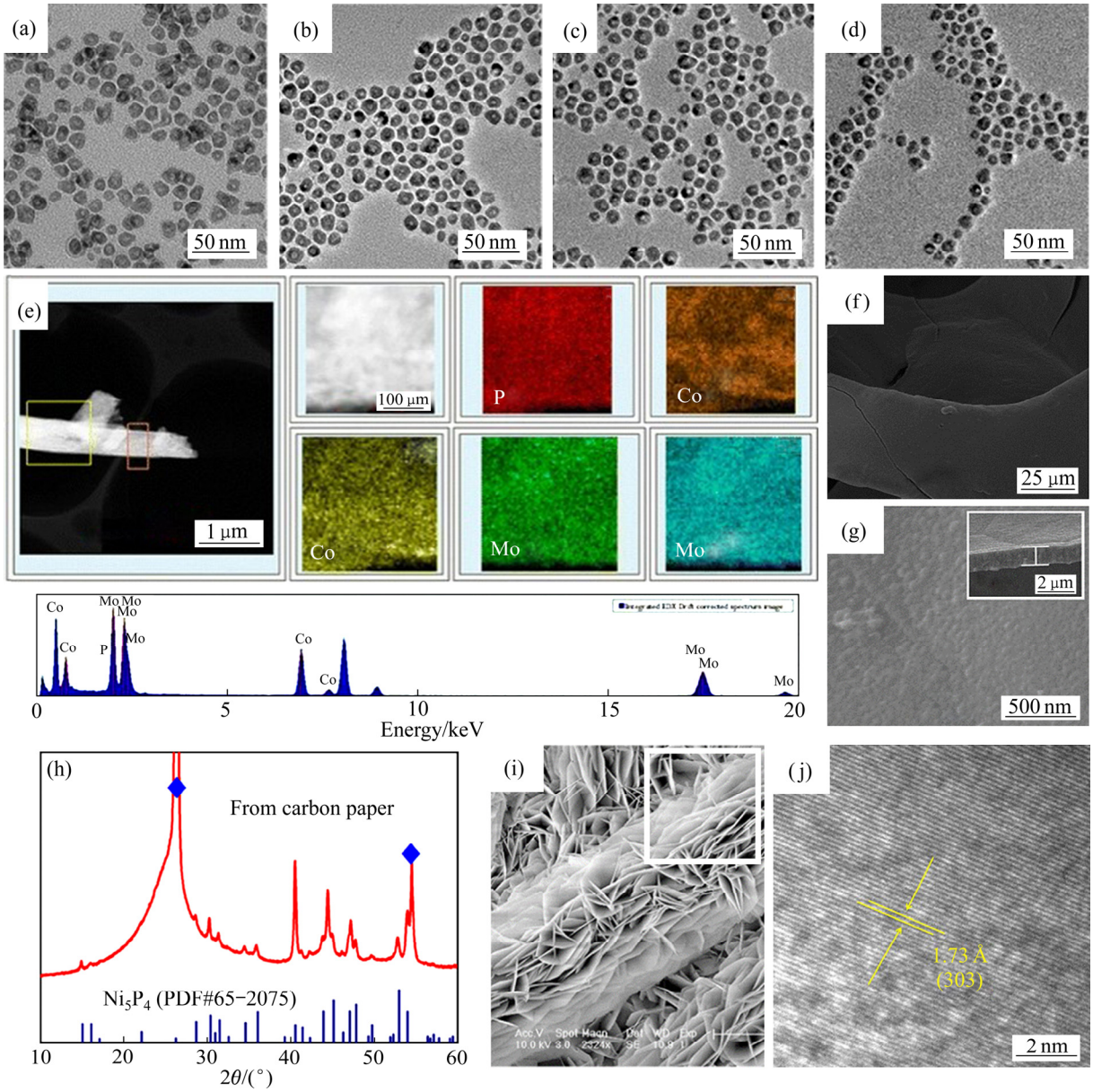

图 5 不同空间尺寸的纳米材料形貌及测试：在 0T(a)、2T(b)、4T(c)和 6T(d)磁场下制备的 Co_2P 空心纳米颗粒的透射电镜图[71]; (e) 磷化温度 600 ℃下 CoMoP 纳米管的扫描透射电镜图及元素分布图[72]; (f), (g) Ni-P/NF 的扫描电镜图(图(g)插图：横截面分析)[73]; (h) S-Ni_5P_4 NPA/CP 的 XRD 图谱[74]; (i) S-Ni_5P_4 NPA/CP 的扫描电镜图(插图：高分辨扫描电镜图)[74]; (j) S-Ni_5P_4 NPA/CP 的高分辨透射电镜图[74]

Fig. 5 Morphologies and measurements of nano materials with different space sizes: TEM images of Co2P hollow NPs prepared at 0T (a), 2T (b), 4T (c) and 6T (d) magnetic fields[71]; (e) STEM-EDX elemental mapping images, CoMoP-600 nanotubes[72]; (f), (g) SEM image, Ni-P/NF (Figure (g) inset: cross-section analysis)[73]; (h) XRD pattern of S-Ni_5P_4 NPA/CP[74]; (i) SEM image, S-Ni_5P_4 NPA/CP (Figure inset: high-magnification SEM image)[74]; (j) HRTEM image, S-Ni_5P_4 NPA/CP[74]

沉积法在泡沫镍上制备 2D Ni-P/NF 镍磷合金薄膜(见图 5(f)~(g))，通过对其性能测试，得出 Ni-P/NF 是一种高效催化剂的结论。在 1 mol/L KOH 溶液中电流密度达到 10 mA/cm^2 时，过电位为 80 mV，并且 Ni-P/NF 在碱性介质中具有很强的耐久性。尽管科研人员对零维/一维/二维材料进行了大量研究，但其仍受制备繁琐和易自聚集限制，因此，具有更高比表面积的三维结构(3D)受到了广泛关注。CHANG 等[74]在碳纸上生长 3D S-Ni_5P_4 NPA/CP 纳米板阵列(见图 5(h)~(j))。与磷化镍和硫化镍相比，3D S-Ni_5P_4 NPA/CP 纳米板阵列有较大的比表面，有利于硫和磷相互调节电子性能。电流密度为 10

mA/cm^2 和 100 mA/cm^2，过电位分别为 56 mV 及 104 mV，Tafel 斜率仅为 43.6 mV/dec。PI 等[75]在碳维布上制备了自立多孔的 WP_2/CC 纳米片阵列，由于其独特的三维结构，因此，有显著的催化性能以和较高的稳定性。

2.2　界面调控

引入空位缺陷是调控 TMPs 催化性能的有效办法，空位缺陷的存在改变了局域的原子结构，从而引起电子结构的变化，增加活性位点，降低了 HER 的反应能垒[76−78]。KWONG 等[79]首次报道了 Fe 空位缺陷来调节磷化铁(FeP)的电子结构，其中 Mg 作为“牺牲掺杂剂”引入 FeP 中，通过化学浸出产生了 Vc-FeP 薄膜。根据计算表明，原始 FeP 最活跃的位点具有ΔG_{H^*}=0.16 eV。添加 Mg 会使ΔG_{H^*}降低至 0.05 eV，这表明氢相互作用更强。对于 Vc-FeP，氢相互作用进一步提高到ΔG_{H^*}=0.02 eV(见图 6(a))。与 FeP 和 Mg-FeP 相比，Vc-FeP 中铁空位在磷化物空位中产生了相对富 P 的环境。其中 P 带有部分负电荷，促进质子捕获，保持较好的析氢活性(见图 6(b))。CHENG 等[80]对 NiAl 氢氧化物(NiAl-LDH)进行蚀刻和磷化，形成独特多孔结构的纳米片($NiAl_\delta P$)(见图 6(c))。从图 6(d)中可以清晰观察到大量的原子空位，该空位缺陷有利于电解质的接触渗

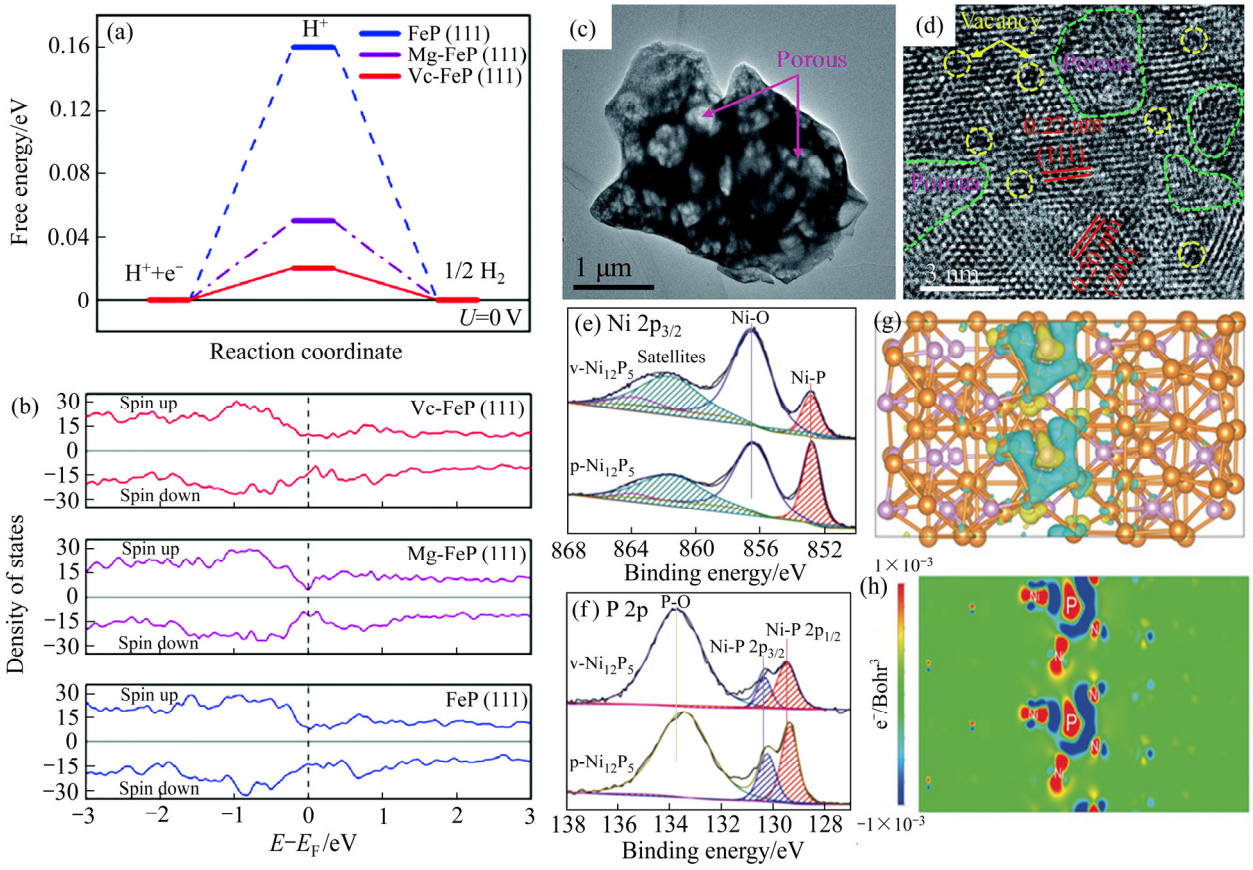

图 6　阴离子和阳离子空位缺陷的纳米材料形貌及理论计算：(a) 电压 U=0 V、pH=0 时相对于标准氢电极所计算出 FeP、Mg-FeP 和 Vc-FeP 的自由能[79]；(b) FeP、Mg-FeP 和 Vc-FeP 表面的态密度(垂直虚线表示费米能级)[79]；(c) $NiAl_\delta P$ 纳米片的的透射电镜图[80]；(d) $NiAl_\delta P$ 纳米片的高分辨透射电镜图[80]；(e)，(f) v-$Ni_{12}P_5$ 的 Ni 2p 和 P 2p 谱[81]；(g) v-$Ni_{12}P_5$ 中电子分布(黄色区域表示电子积累，青色表示电子耗尽)[81]；(h) v-$Ni_{12}P_5$ 的二维电荷差等值面(红色为富电子区，蓝色为缺电子区)[81]

Fig. 6　Morphologies and theoretical calculation of nano materials with anionic and cationic vacancy defects: (a) Calculated free energy of FeP, Mg-FeP and Vc-FeP relative to that of standard hydrogen electrode at voltage U=0 V and pH=0[79]; (b) Density of states of FeP, Mg-FeP and Vc-FeP surfaces (Vertical dotted line represents Fermi level)[79]; (c) TEM image of $NiAl_\delta P$ nanosheets[80]; (d) HRTEM image of $NiAl_\delta P$ nanosheets[80]; (e), (f) Ni 2p and P 2p spectra of v-$Ni_{12}P_5$[81]; (g) Electron distribution (Yellow area indicating electron accumulation while cyan meaning electron depletion)[81]; (h) Two-dimensional charge difference isosurface of v-$Ni_{12}P_5$ (Red electron-rich, blue deficient)[81]

透和电子转移。目前，采用阳离子空位缺陷调控磷化物的电催化性能已经有较为完善的研究，而TMPs中阴离子空位缺陷对其电催化性能的影响研究还比较有限。DUAN等[81]在泡沫镍表面上制备了磷空位缺陷的(v-$Ni_{12}P_5$)(见图6(e)~(f))。DFT计算表明，v-$Ni_{12}P_5$内具有大量电子积累，从而在磷化镍晶体中引起了显着的电子再分布(见图6(g)~(h))，极大地提高了析氢催化活性。实验结果与预期一样，在1 mol/L KOH溶液中，产生10 mA/cm^{2}电流密度，需要的过电位为27.7 mV，并且Tafel斜率也较小，仅为30.88 mV/dec。总的来说，无论是引入阳离子空位还是阴离子空位，都可以有效的提高催化活性。由于磷空位可以削弱M(过渡金属)3d和P 2p轨道的杂化，丰富磷空位附近M和磷原子的电子密度，并促进氢原子(H*)的解吸过程[82−85]，因此，对磷空位的探索逐渐成为TMPs空位研究的热点。

异质原子掺杂是从原子尺度上调控TMPs析氢的方法，异质原子的添加破坏了金属磷化物晶格的周期性，引起了局域电子结构的改变，从而优化电荷转移[86−89]。根据原子种类可分为金属掺杂、非金属掺杂、金属−非金属掺杂[90−93]。PAN等[94]合成了Fe、Ni、Mn掺杂的CoP空心多面体(见图7(a))，通过X射线吸收近边结构谱可知，金属原子的掺杂改变了CoP的电子结构，电荷由掺杂的金属原子向Co原子转移(见图7(b)和7(c))。由H吸附自由能可得，原子的掺杂改变了ΔG_{H^*}，其中Ni原子的掺杂最小(−0.03 eV)。因此，Ni原子掺杂CoP的过电位最小。LIU等[95]在钛片上生长了Mn掺杂CoP纳米片阵列(见图7(d))，由于锰的掺杂，削弱了Co和H原子之间的相互作用，因此，增强了吸附态氢原子的脱附。在0.5 mol/L H_2SO_4中产生10 mA/cm^{2}电流密度时，需要的过电位仅为49 mV，Tafel斜率为55 mV/dec；在1 mol/L KOH中，产生相同的电流密度，需要的过电位为76 mV，Tafel斜率为82 mV/dec。ZHANG等[96]将O原子引入MoP、CoP中，增强了它们的固有电导率，拉长了Mo—P和Co—P键，促进电荷的转移，从而获得了优异的HER活性。ZHANG等[97]提出了将N原子同时掺杂在磷化物和载体上，该制备方法利用次磷酸铵分解产生的氨和磷化氢气体与前驱体进行反应，得到N掺杂碳纳米管负载氮掺杂磷化钼催化剂(N-MoP/N-CNT)。N的掺杂调谐了电子结构并且与碳纳米管产生耦合效应，促进了析氢活性(图7(e)~(f))。当电流密度为10 mA/cm^{2}时，过电势为(103±5) mV，低于MoP纳米颗粒的过电势(243 mV)。单一金属和非金属原子掺杂体系无法很好平衡H_2O的吸附和解离，而多种元素之间的协同作用能进一步地优化催化剂对HER中间物种的吸附能，降低HER过电位。XU等[98]设计出了一种Cu和O共掺杂的方法，制备出了CoP纳米线阵列(见图7(g))，金属−非金属的掺杂创造了大量的晶格缺陷，增加了活性位点，O和Cu共掺杂CoP纳米线阵列的催化活性比未掺杂的CoP纳米线阵列提高了近10倍(见图7(h))。对上述文献探讨可知，异质原子掺杂可有效调整电子结构、增强润湿性、降低动能势垒和引入额外的活性位点。近年来，通过掺杂一系列金属原子，它们不仅可以增强电导率，还可以通过调节电子结构来优化氢吸附能。

2.3 材料复合

过渡金属磷化物与导电材料复合，可以提高材料的导电性，且基底与活性组分之间存在协同作用，增强了过渡金属磷化物颗粒的稳定性，削弱团聚现象[99−101]。TANG等[102]在钛箔上制备出了Fe-CoP/Ti纳米阵列。对结果分析，钛箔的存在提高活性物间的导电性。令人惊讶的是，这种Fe-CoP/Ti对$NaBH_4$的水解脱氢也具有很高的活性。相比于其他基底，碳布(CC)具有价格低廉，高导电性以及良好的的柔韧性等特点。LIANG等[103]通过低温磷酸化，在CC上开发了自支撑的FeP纳米棒阵列(见图8(a)和(b))，在酸性溶液中FeP NAs/CC表现出高催化活性，仅需58 mV的过电势即可提供10 mA/cm^{2}的电流密度，塔菲尔斜率为45 mV/dec。同时，TIAN等[104]通在CC上直接生长FeP纳米颗粒(FeP/CC)。在大电流密度下(100 mA/cm^2)，需要的过电位仅为108 mV(见图8(c))。泡沫镍具有较大的比表面积，可以加速离子的扩散，促进电子转移率。TONG[105]通过在氮掺杂碳包覆的泡沫镍上，生长出三维纳米片(NiCoP/NF@NC)。毫无疑问，在碱性溶液中，当电流密度为10 mA/cm^{2}时，过电位仅为31.8 mV，塔菲尔斜率62.3 mV/dec。石墨烯充当底物，不仅可以避免颗粒聚集，而且还可以促进电子转移。WU等[106]通过高温磷化制备出了氧化石墨烯负载的磷化钼纳米颗粒(MoP-RGO)(见图8(d))。

结果表明，900℃下制备的 MoP-RGO 展现出稳定的析氢性能(见图 8(e)~(f))。RIYAJUDDIN 等[107]将泡沫镍、石墨烯和碳纳米管三者复合作为导电基底，与 Ni_2P-CuP_2 异质结构合成出超亲水双金属磷化物(见图 8(g))。该基底改善了导电性，加速了电子传输，并且提供了有利的亲水性和憎水性表面，在电

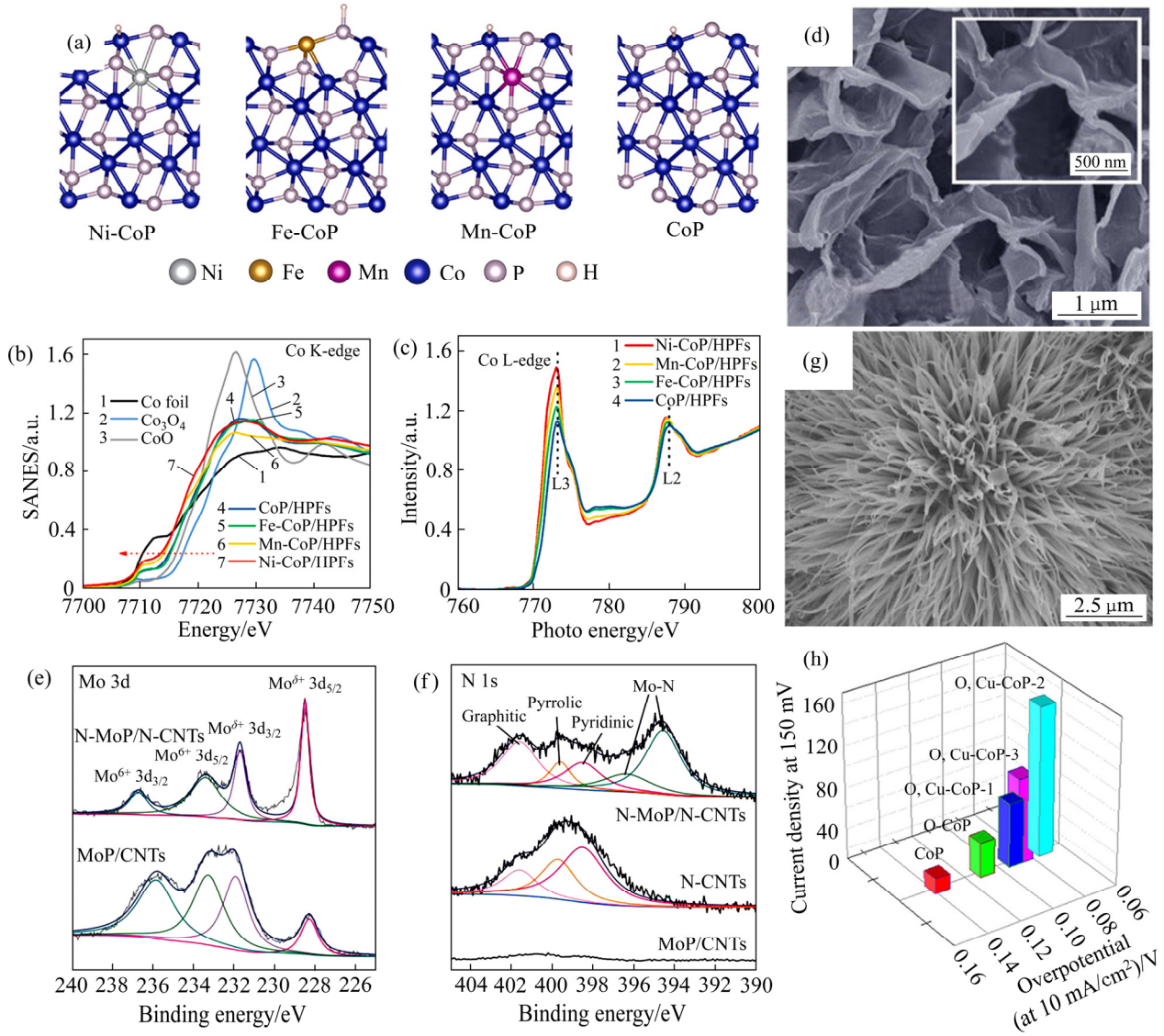

图 7　金属与非金属掺杂的纳米材料形貌及催化性能测试：(a) 理论计算 Fe-CoP、Ni-CoP 和 Mn-CoP 的结构[94]；(b) Co 箔、Co_3O_4、CoO、CoP/HPFs、Fe-CoP /HPFs、Mn-CoP/HPFs 和 Ni-CoP/HPFs 的 Co-K 边 XANES 光谱[94]；(c) CoP/HPFs、Fe-CoP/HPFs、Mn-CoP/HPFs 和 Ni-CoP/HPFs 的 Co-L 边的 XANES 光谱[94]；(d) Mn-CoP/Ti 的扫描电镜图(插图：高分辨扫描电镜图)[95]；(e) N-MoP/N-CNT 和 MoP/N-CNT 的 Mo 3d 光谱[97]；(f) N-MoP/N-CNT、N-CNTs 和 MoP/N-CNT 的 N 1s 光谱[97]；(g) N-MoP/N-CNT 的 SEM 像[98]；(h) 在 1 mol/L KOH 电解液中以 Ag/AgCl 为参比电极(RE)、石墨棒为对电极(CE)对 O, Cu-CoP、O-CoP 和 CoP 进行 IR 校正的极化曲线[98]

Fig. 7　Morphologies and catalytic properties of metal and non-metal doped nano materials: (a) Theoretical calculation of structures of Fe-CoP, Ni-CoP and Mn-CoP[94]; (b) XANES spectra at Co K-edge of Co foil, Co_3O_4, CoO, CoP/HPFs, Fe-CoP/HPFs, Mn-CoP/HPFs and Ni-CoP/HPFs[94]; (c) XANES spectra at Co L-edge of CoP/HPFs, Fe-CoP/HPFs, Mn-CoP/HPFs and Ni-CoP/HPFs[94]; (d) SEM image, Mn-CoP/Ti (Figure inset: high-magnification SEM image)[95]; (e) Mo 3d spectra of N-MoP/N-CNTs and MoP/CNTs[97]; (f) N 1s spectra of N-MoP/N-CNTs, N-CNTs and MoP/CNT[97]; (g) SEM image, N-MoP/N-CNT[98]; (h) IR-corrected polarization curves of O, Cu-CoP nanowire, O-CoP nanowire and CoP nanowire electrodes in 1 mol/L KOH electrolyte using Ag/AgCl as reference electrode (RE) and graphite bar as counter electrode (CE)[98]

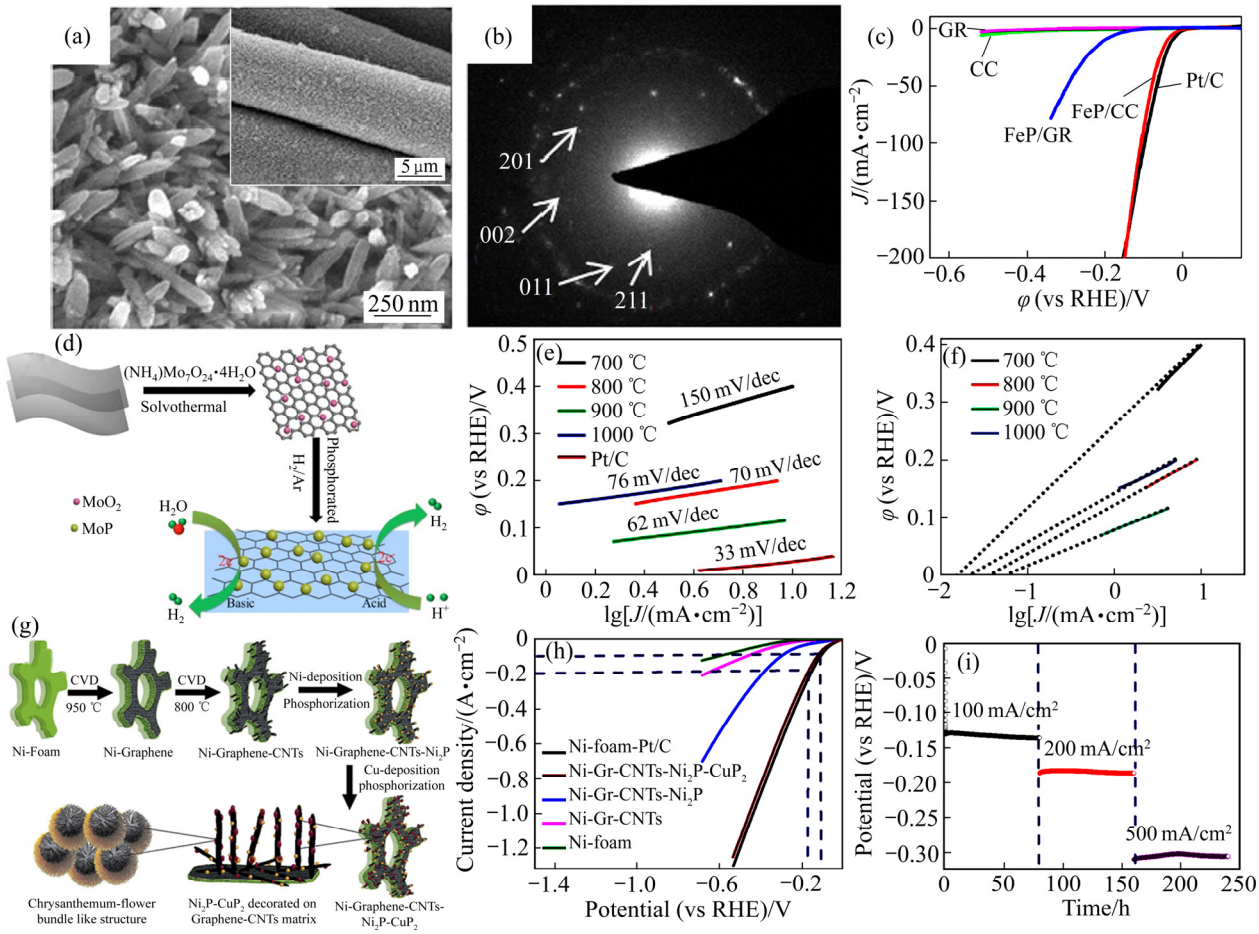

图 8 导电材料复合的纳米材料形貌及催化性能测试：(a) FeP NAs/CC 的扫描电镜图(插图：低分辨电镜图)[103]；(b) FeP 纳米棒的的选区电子衍射谱图[103]；(c) 碳布、石墨棒、FeP/CC、FeP/GR 以及 Pt/C 在 0.5 mol/L H_2SO_4 中扫速为 2 mV/s 时的极化曲线[104]；(d) MoP-RGO 的示意图[106]；(e) 在 0.5 mol/L H_2SO_4 溶液中以 5 mV/s 的扫描速率获得不同磷化温度 MoP-RGO 及 Pt/C 对应的 Tafel 斜率[106]；(f) 在 0.5 mol/L H_2SO_4 溶液中以 5 mV/s 的扫描速率获得不同磷化温度 MoP-RGO 对应的交换电流密度[106]；(g) 泡沫镍−石墨烯−碳纳米−Ni_2P−CuP_2 合成示意图[107]；(h) 泡沫镍、泡沫镍−石墨烯−碳纳米管、泡沫镍−石墨烯−碳纳米管−Ni_2P、泡沫镍−石墨烯−碳纳米管−Ni_2P−CuP_2、以及泡沫镍−Pt/C 在 0.5 mol/L H_2SO_4 中扫速为 5 mV/s 时的极化曲线[107]；(i) 分别在 100、200 和 500 mA/cm^2 恒电流密度下对 Ni-graphene-CNTs-Ni_2P-CuP_2 进行长期稳定性试验[107]

Fig. 8 Morphologies and catalytic properties of conductive composite nano materials: (a) SEM image, FeP NAs/CC (Figure inset: low-magnification SEM image)[93]; (b) SAED pattern taken from FeP nanorod[93]; (c) Polarization curves, CC, GR, FeP/CC, FeP/GR and Pt/C in 0.5 mol/L H_2SO_4 at 2 mV/s[94]; (d) Schematic illustration for synthesis of MoP-RGO[95]; (e) Tafel slopes of MoP-RGO and Pt/C at different phosphating temperatures obtained in 0.5 mol/L H_2SO_4 solution at scanning rate of 5 mV/s[95]; (f) Exchange current densities of MoP-RGO at different phosphating temperatures obtained in 0.5 mol/L H_2SO_4 solution at scanning rate of 5 mV/s[95]; (g) Schematic illustration for synthesis, NF-RGO-CNTs-Ni_2P-CuP_2[96]; (h) NF, NF-RGO-CNTs, NF-RGO-CNTs-Ni_2P, NF-RGO-CNTs-Ni_2P-CuP_2 and Ni-Pt/C in 0.5 mol/L H_2SO_4 at 5 mV/s[96]; (i) Long-term stability of Ni-graphene-CNTs-Ni_2P-CuP_2 tested at constant current density of 100 mA/cm^2, 200 mA/cm^2 and 500 mA/cm^2, respectively[96]

极−电解质界面形成低欧姆电阻路径，促进其更快地去除气泡。在酸性介质中的电流密度为 10 mA/cm^{2}时显示 12 mV 的超低电势(见图 8(h))。此外，在 500 mA/cm^2 的高电流密度下可持续至少 10 d(见图 8(i))。在性能测试过程中，通过黏合剂将催化材料与导电载体结合，然而，此种方法，易造成催化

材料从电极上脱落，不利于电子转移，严重制约了催化活性和稳定性。因此，直接在导电基材上生长的 TMPs 被认为是潜在的电催化剂候选者。

表 3 总结了不同过渡金属磷化物的析氢性能，从表中清楚看出，磷化物在析氢催化剂中展现出优异性能。为了提高催化活性，可以从如下几个角度深入：首先，引入贵金属来降低催化剂的过电位。例如，Ru-Ni2P/NiO/NF 的析氢过电位仅为 12 mV。其次，可以考虑将制备材料在载体上原位生长，这样优势在于，一方面可以提高导电性，另一方面，有效避免粘结剂带来的负面效应。最后，鉴于不同金属之间的协同效应，可以考虑双金属或者多金属体系。

3　结论与展望

为了聚焦“碳达峰、碳中和”绿色低碳的发展目标，这就需要持续提升能源利用效率，加快能源消费方式转变。然而，电解水制氢恰好可以有效缓解能源转换这一棘手问题。过渡金属磷化物凭借其独特的催化活性，被科研人员广泛研究。目前，科研工作者主要从形貌设计(结构、维度、高活性表面暴露)、界面调控(空位缺陷、异质原子掺杂)、材料复合等手段提高 HER 催化性能，虽然收到了一定的成效，但电解水制氢的市场化，仍然任重而道远。未来可考虑从如下几个方面进一步研究。

1) 关注原子级反应机理。当前，电解水析氢的最大困境在于人们无法从原子级上掌握电解水的反应过程。为了阐明机理，研究人员可以采用理论计算和实验分析相结合的方法，之所以加入理论计算，原因在于密度泛函理论可以鉴别中间产物和预测实际活性位点。

2) 探索全解水性能。研究表明，过渡金属磷化物在酸性条件下比碱性显示出更稳定的析氢性能。

表 3　典型报道过渡金属磷化物的析氢性能

Table 3　HER performance of typical reported transition metal phosphide

Method	Catalyzer	Feature	Overpotential/mV @10 mA·cm^{-2}	Tafel/ (mV·dec^{-1})	Electrolyte	Ref.
Shape design	Ni-Cu-P	Dendrite shape	120	69	1 mol/L KOH	[37]
	Ru-Ni_2P/NiO/NF	Petal shape	12	22.6	1 mol/L KOH	[58]
	$Ni_{12}P_5$	Hollow sphere shape	144	46	0.5 mol/L H_2SO_4	[64]
	CoPS/CP	Sea urchin shape	48	42.6	0.5 mol/L H_2SO_4	[65]
Dimensional regulation	Co_2P	0D	131	36	1 mol/L KOH	[71]
	CoMoP	1D	220	136	0.5 mol/L H_2SO_4	[72]
	Ni-P/NF	2D	80	50	1 mol/L KOH	[73]
	S-Ni_5P_4 NPA/CP	3D	56	43.6	0.5 mol/L H_2SO_4	[74]
Vacancy defect	MoP	MoP	104	50	1 mol/L KOH	[76]
	FeP	Fe	65	49	0.5 mol/L H_2SO_4	[79]
	NiAlP	Al	35	38	0.5 mol/L H_2SO_4	[80]
	$Ni_{12}P_5$	P	27.7	30.8	1 mol/L KOH	[81]
Element doping	CoP/HTPs	Ni	92	71	1 mol/L KOH	[94]
	CoP/Ti	Mn	49	55	0.5 mol/L H_2SO_4	[95]
	MoP/N-CNTs	N	103	42	0.5 mol/L H_2SO_4	[97]
	CoP	Cu, O	85	62.2	1 mol/L KOH	[98]
Composite material	Fe-CoP/Ti	Titanium foil	78	75	1 mol/L KOH	[102]
	FeP NAs/CC	Carbon cloth	58	45	0.5 mol/L H_2SO_4	[103]
	MoP/RGO	Graphene	117	62	0.5 mol/L H_2SO_4	[106]
	Ni_2P-CuP_2	NF graphene nanotubes	12	41	0.5 mol/L H_2SO_4	[107]

然而，在实际的工业化应用中，所需要的催化剂应具备全 pH(0~14)条件下都能展现出稳定性能。因此，社会迫切需要发展全 pH 中稳定且具有良好催化活性的 TMPs。

3) 设计特定空位缺陷。随着对缺陷的日益关注，缺陷工程已成为电催化剂设计的常用策略。研究人员应重视如何引入特定缺陷以及多种缺陷的协同效应对提高析氢反应的促进作用。

4) 考虑 TMPs 在外界场下的制备。随着磁场、热场、声场、光场等理论体系的完善，学者们可以探究在外界场的环境下，所制备过渡金属磷物析氢性能的变化。

随着科学的进步与发展，相信在不远的将来，过渡金属磷化物在电解水析氢反应中存在的难点问题会逐步得到改善。遥想未来，氢能必将全方位地应用在动力设备上以及高效的提高人类生活水平中。

REFERENCES

[1] VESBORG P C K, SEGER B, CHORKENDORFF I. Recent development in hydrogen evolution reaction catalysts and their practical implementation[J]. The Journal of Physical Chemistry Letters, 2015, 6(6): 951−957.

[2] CHUA C K, PUMERA M. Susceptibility of FeS_2 hydrogen evolution performance to sulfide poisoning[J]. Electrochemistry Communications, 2015, 58: 29−32.

[3] 梁叔全, 程一兵, 方国赵, 等. 能源光电转换与大规模储能二次电池关键材料的研究进展[J]. 中国有色金属学报, 2019, 29(9): 2064−2114.
LIANG Shu-quan, CHENG Yi-bing, FANG Guo-zhao, et al. Research progress of key materials for energy photoelectric conversion and large-scale energy storage secondary batteries[J]. The Chinese Journal of Nonferrous Metals, 2019, 29(9): 2064−2114.

[4] 贺亚维, 吴世照, 李玉儒, 等. Pt-WC/Mnt三元纳米复合材料的制备及其电催化性能[J]. 中国有色金属学报, 2020, 30(2): 392−400.
HE Ya-wei, WU Shi-zhao, LI Yu-ru, et al. Preparation of Pt-WC/Mnt nano-composite and its electrocatalytic activity[J]. The Chinese Journal of Nonferrous Metals, 2020, 30(2): 392−400.

[5] GAO H, YUE H H, QI F, et al. Few-layered ReS_2 nanosheets grown on graphene as electrocatalyst for hydrogen evolution reaction[J]. Rare Metals, 2018, 37(12): 1014−1020.

[6] XIE W F, LI Z H, SHAO M F, et al. Layered double hydroxide-based core-shell nanoarrays for efficient electrochemical water splitting[J]. Frontiers of Chemical Science and Engineering, 2018, 12(3): 537−554.

[7] ZHENG L L, XIAO X Y, LI Y, et al. Enhanced photocatalytic activity of TiO_2 nanoparticles using WS_2/g-C_3N_4 hybrid as co-catalyst[J]. Transactions of Nonferrous Metals Society of China, 2017, 27(5): 1117−1126.

[8] DING W L, CAO Y H, LIU H, et al. In situ growth of NiSe@$Co_{0.85}$Se heterointerface structure with electronic modulation on nickel foam for overall water splitting[J]. Rare Metals, 2021, 40(6): 1373−1382.

[9] ZOU X X, ZHANG Y. Noble metal-free hydrogen evolution catalysts for water splitting[J]. Chemical Society Reviews, 2015, 44(15): 5148−5180.

[10] TRANCIK J E. Renewable energy: Back the renewables boom[J]. Nature, 2014, 507(7492): 300−302.

[11] LIU Y R, HU W H, LI X, et al. Facile one-pot synthesis of CoS_2-MoS_2/CNTs as efficient electrocatalyst for hydrogen evolution reaction[J]. Applied Surface Science, 2016, 384: 51−57.

[12] ZHOU B W, LI J W, ZHANG X, et al. Engineering P-doped Ni_3S_2-NiS hybrid nanorod arrays for efficient overall water electrolysis[J]. Journal of Alloys and Compounds, 2021, 862: 158391.

[13] WANG J, XU F, JIN H Y, et al. Non-noble metal-based carbon composites in hydrogen evolution reaction：Fundamentals to applications[J]. Advanced Materials, 2017, 29(14): 1605838.

[14] YANG C F, ZHAO R, XIANG H, et al. Ni-activated transition metal carbides for efficient hydrogen evolution in acidic and alkaline solutions[J]. Advanced Energy Materials, 2020, 10(37): 2002260.

[15] ZHENG L, ZHANG W, GAO B, et al. One-pot synthesis of few-layered molybdenum disulfide anchored on N, S-codoped carbon for enhanced hydrogen generation[J]. Materials Today Energy, 2021, 19: 100600.

[16] JIN H Y, GU Q F, CHEN B, et al. Molten salt-directed catalytic synthesis of 2D layered transition-metal nitrides for efficient hydrogen evolution[J]. Chem, 2020, 6(9): 2382−2394.

[17] KIM M, LEE B, JU H, et al. Reducing the barrier energy of

self-reconstruction for anchored cobalt nanoparticles as highly active oxygen evolution electrocatalyst[J]. Advanced Materials, 2019, 31(32): 1901977.

[18] ZHAO X, XUE Z, CHEN W, et al. Eutectic synthesis of high-entropy metal phosphides for electrocatalytic water splitting[J]. ChemSusChem, 2020, 13(8): 2038−2042.

[19] SHI Y M, ZHANG B. Recent advances in transition metal phosphide nanomaterials: Synthesis and applications in hydrogen evolution reaction[J]. Chemical Society Reviews, 2016, 45(6): 1529−1541.

[20] YUN G N, AHN S J, TAKAGAKI A, et al. Hydrodeoxygenation of γ-valerolactone on bimetallic NiMo phosphide catalysts[J]. Journal of Catalysis, 2017, 353: 141−151.

[21] XUAN Y, QUAN H, SHEN Z, et al. Band-gap and charge transfer engineering in red phosphorus-based composites for enhanced visible-light-driven H_2 evolution[J]. Chemistry—A European Journal, 2020, 26(10): 2285−2292.

[22] ZHANG S J, SONG L M, WU X Q, et al. Synthesis of high-dispersed $NiCoP/SiO_2$ and hydrodesulfurization performance[J]. Vacuum, 2014, 108: 45−48.

[23] MCENANEY J M, CROMPTON J C, CALLEJAS J F, et al. Amorphous molybdenum phosphide nanoparticles for electrocatalytic hydrogen evolution[J]. Chemistry of Material, 2014, 26(16): 4826−4831.

[24] POPCZUN E J, MCKONE J R, READ C G, et al. Nanostructured nickel phosphide as an electrocatalyst for the hydrogen evolution reaction[J]. Journal of the American Chemical Society, 2013, 135(25)：9267−9270.

[25] ZHANG H, HA D H, HOVDEN R, et al. Controlled synthesis of uniform cobalt phosphide hyperbranched nanocrystals using tri-*n*-octylphosphine oxide as a phosphorus source[J]. Nano Letters, 2011, 11(1): 188−197.

[26] ZHENG X, YUAN S, TIAN Z, et al. One-pot synthesis of hollow nickel phosphide nanoparticles with tunable void sizes using triphenylphosphine[J]. Materials Letters, 2009, 63(27): 2283−2285.

[27] ZHENG X, YUAN S, TIAN Z, et al. Nickel/nickel phosphide core-shell structured nanoparticles: Synthesis, chemical, and magnetic architecture[J]. Chemistry of Materials, 2009, 21(20): 4839−4845.

[28] WANG J, CHEN H, FU Y, et al. Highly active Ni_2P/SiO_2 catalysts phosphorized by triphenylphosphine in liquid phase for the hydrotreating reactions[J]. Applied Catalysis B: Environmental, 2014, 160/161: 344−355.

[29] PAN Y, HU W H, LIU D P, et al. Carbon nanotubes decorated with nickel phosphide nanoparticles as efficient nanohybrid electrocatalysts for the hydrogen evolution reaction[J]. Journal of Materials Chemistry A, 2015, 3(24): 13087−13094.

[30] LI X, LIU W, ZHANG M, et al. Strong metal-phosphide interactions in core-shell geometry for enhanced electrocatalysis[J]. Nano Letters, 2017, 17(3): 2057−2063.

[31] DU Y, QU H, LIU Y, et al. Bimetallic CoFeP hollow microspheres as highly efficient bifunctional electrocatalysts for overall water splitting in alkaline media[J]. Applied Surface Science, 2019, 465: 816−823.

[32] MA Y Y, WU C X, FENG X J, et al. Highly efficient hydrogen evolution from seawater by a low-cost and stable CoMoP@C electrocatalyst superior to Pt/C[J]. Energy & Environmental Science, 2017, 10(3): 788−798.

[33] LU X F, YU L, LOU X W D. Highly crystalline Ni-doped FeP/carbon hollow nanorods as all-pH efficient and durable hydrogen evolving electrocatalysts[J]. Science Advances, 2019, 5(2): eaav6009.

[34] WANG X, NA Z, YIN D, et al. Phytic acid-assisted formation of hierarchical porous CoP/C nanoboxes for enhanced lithium storage and hydrogen generation[J]. ACS Nano, 2018, 12(12): 12238−12246.

[35] CHENG J, LI T, ULLAH S, et al. Giant magnetocaloric effect in nanostructured Fe-Co-P amorphous alloys enabled through pulse electrodeposition[J]. Nanotechnology, 2020, 31(38): 385704.

[36] PEI Y, YANG Y, ZHANG F, et al. Controlled electrodeposition synthesis of Co-Ni-P film as a flexible and inexpensive electrode for efficient overall water splitting[J]. ACS Applied Materials & Interfaces, 2017, 9(37): 31887−31896.

[37] CAO M, XUE Z, NIU J J, et al. Facile electrodeposition of Ni-Cu-P dendrite nanotube films with enhanced hydrogen evolution reaction activity and durability[J]. ACS Applied Materials & Interfaces, 2018, 10(41): 35224−35233.

[38] YANG F, YANG S, NIU Q, et al. Fabrication of a 3D self-supporting $Ni\text{-}P/Ni_2P/CC$ composite and its robust hydrogen evolution reaction properties in alkaline solution[J]. New Journal of Chemistry, 2020, 44(20): 8183−8190.

[39] LIU Y, WANG L, FENG H, et al. Microemulsion-assisted self-assembly and synthesis of size-controlled porphyrin nanocrystals with enhanced photocatalytic hydrogen evolution[J]. Nano Letters, 2019, 19(4): 2614−2619.

[40] ADESUJI E T, KHALIL L, VIDEA M, et al. From nano to macro: Hierarchical platinum superstructures synthesized

using bicontinuous microemulsion for hydrogen evolution reaction[J]. Electrochimica Acta, 2020, 354: 136608.

[41] JIANG Y, WANG D, PAN Z, et al. Microemulsion-mediated hydrothermal synthesis of flower-like MoS_2 nanomaterials with enhanced catalytic activities for anthracene hydrogenation[J]. Frontiers of Chemical Science and Engineering, 2018, 12(1): 32−42.

[42] MOTOS-PÉREZ B, UZIO D, AYMONIER C, et al. Preparation of nickel phosphide hydrodesulfurization catalysts assisted by supercritical carbon dioxide[J]. Chem Cat Chem, 2015, 7(21): 3441−3444.

[43] TIAN S, LI X, WANG A , et al. Facile preparation of Ni_2P with a sulfur-containing surface layer by low-temperature reduction of $Ni_2P_2S_6$[J]. Angewandte Chemie International Edition, 2016, 55(12): 4030−4034.

[44] ZOU X X, WU Y Y, LIU Y P, et al. In situ generation of bifunctional, efficient Fe-based catalysts from mackinawite iron sulfide for water splitting[J]. Chem, 2018, 4(5): 1139−1152.

[45] LIU J L, ZHENG Y, WANG Z Y, et al. Free-standing single-crystalline NiFe-hydroxide nanoflake arrays: A self-activated and robust electrocatalyst for oxygen evolution[J]. Chemical Communications, 2018, 54(5): 463−466.

[46] LONG J Y, GONG Y, LIN J H. Metal-organic framework derived Co_9S_8@CoS@CoO@C nanoparticles as efficient electro-and photo-catalysts for the oxygen evolution reaction[J]. Journal of Materials Chemistry A, 2017, 5(21): 10495−10509.

[47] JIANG P, LIU Q, SUN X. NiP_2 nanosheet arrays supported on carbon cloth: An efficient 3D hydrogen evolution cathode in both acidic and alkaline solutions[J]. Nanoscale, 2014, 6(22): 13440−13445.

[48] ZHANG Y, WANG Y, WANG T T, et al. Heterostructure of 2D CoP nanosheets/1D carbon nanotubes to significantly boost the alkaline hydrogen evolution[J]. Advanced Materials Interfaces, 2020, 7(2): 1901302.

[49] ZHANG S C, XIONG T, TANG X F, et al. Engineering inner-porous cobalt phosphide nanowire based on controllable phosphating for efficient hydrogen evolution in both acidic and alkaline conditions[J]. Applied Surface Science, 2019, 481(15): 1524−1531.

[50] YU L, MISHRA I K, XIE Y L, et al. Ternary $Ni_{2(1-x)}Mo_{2x}P$ nanowire arrays toward efficient and stable hydrogen evolution electrocatalysis under large-current-density[J]. Nano Energy, 2018, 53: 492−500.

[51] ZHENG H Y, HUANG X B, WU Z Y, et al. Controlled synthesis of 3D flower-like Ni_2P composed of mesoporous nanoplates for overall water splitting[J]. Chemistry—An Asian Journal, 2017, 12(22): 2956−2961.

[52] HUANG J Y, CHEN M T, ZHANG X W, et al. P-doped 3D graphene network supporting uniformly vertical MoS_2 nanosheets for enhanced hydrogen evolution reaction[J]. International Journal of Hydrogen Energy, 2020, 45(7): 4043−4053.

[53] BACH L G, THI M L N, SON N T, et al. Mesoporous gold nanoparticles supported cobalt nanorods as a free-standing electrochemical sensor for sensitive hydrogen peroxide detection[J]. Journal of Electroanalytical Chemistry, 2019, 848: 113359.

[54] QAZI U Y, JAVAID R, TAHIR N, et al. Design of advanced self-supported electrode by surface modification of copper foam with transition metals for efficient hydrogen evolution reaction[J]. International Journal of Hydrogen Energy, 2020, 45(58): 33396−33406.

[55] YOON T, KIM K S. One-step synthesis of CoS-doped β-$Co(OH)_2$@Amorphous MoS_{2+x} hybrid catalyst grown on nickel foam for high-performance electrochemical overall water splitting[J]. Advanced Functional Materials, 2016, 26(41): 7386−7393.

[56] TIAN J Q, LIU Q, ASIRI A M, et al. Self-supported nanoporous cobalt phosphide nanowire arrays: An efficient 3D hydrogen-evolving cathode over the wide range of pH 0−14[J]. Journal of the American Chemical Society, 2014, 136(21): 7587−7590.

[57] LIANG Y H, LIU Q, LUO Y L, et al. $Zn_{0.76}Co_{0.24}S/CoS_2$ nanowires array for efficient electrochemical splitting of water[J]. Electrochimica Acta, 2016, 190: 360−364.

[58] YANG C, GAO M Y, ZHANG Q B, et al. In-situ activation of self-supported 3D hierarchically porous Ni_3S_2 films grown on nanoporous copper as excellent pH-universal electrocatalysts for hydrogen evolution reaction[J]. Nano Energy, 2017, 36: 85−94.

[59] CHIA X Y, PUMERA M. Characteristics and performance of two-dimensional materials for electrocatalysis[J]. Nature Catalysis, 2018, 1(12): 909−921.

[60] 杨玉美, 石倩玉, 于雅娜, 等. ZIF-67 衍生纳米磷化钴催化硼氢化钠水解制氢[J]. 中国有色金属学报, 2020, 30(8): 1982−1989.
YANG Yu-mei, SHI Qian-yu, YU Ya-na, et al. ZIF-67 derived cobalt phosphides nanocatalysts for catalytic hydrolysis of sodium borohydride to generate hydrogen[J]. The Chinese Journal of Nonferrous Metals, 2020, 30(8):

1982−1989.

[61] 曹晓兰, 隋 升, 李 冰, 等. 还原剂浓度对原位沉积铂纳米线催化层结构和性能的影响[J]. 中国有色金属学报, 2020, 30(3): 604−611.
CAO Xiao-lan, SUI Sheng, LI Bing. Effects of reducing agent concentrations on structure and properties of in-situ deposited platinum nanowires catalytic layer[J]. The Chinese Journal of Nonferrous Metals, 2020, 30(3): 604−611.

[62] ZHANG H M, WU X Y, CHEN C, et al. Spontaneous ruthenium doping in hierarchical flower-like Ni_2P/NiO heterostructure nanosheets for superb alkaline hydrogen evolution[J]. Chemical Engineering Journal, 2021, 417: 128069.

[63] WAN S H, QI J, ZHANG W, et al. Hierarchical Co(OH)F superstructure built by low-dimensional substructures for electrocatalytic water oxidation[J]. Advanced Materials, 2017, 29(28): 1700286.

[64] CHANG J F, LI S T, LI G Q, et al. Monocrystalline $Ni_{12}P_5$ hollow spheres with ultrahigh specific surface areas as advanced electrocatalysts for the hydrogen evolution reaction[J]. Journal of Materials Chemistry A, 2016, 4(25): 9755−9759.

[65] CHANG J F, OUYANG Y X, GE J J, et al. Cobalt phosphosulfide in the tetragonal phase: A highly active and durable catalyst for the hydrogen evolution reaction[J]. Journal of Materials Chemistry A, 2018, 6(26): 12353−12360.

[66] YANG H, ZHANG Y, HU F, et al. Urchin-like CoP nanocrystals as hydrogen evolution reaction and oxygen reduction reaction dual-electrocatalyst with superior stability[J]. Nano Letters, 2015, 15(11): 7616−7620.

[67] CHEN X, CHENG M, CHEN D, et al. Shape-controlled synthesis of Co_2P nanostructures and their application in supercapacitors[J]. ACS Applied Materials & Interfaces, 2016, 8(6): 3892−3900.

[68] TAN C, CAO X, WU X J, et al. Recent advances in ultrathin two-dimensional nanomaterials[J]. Chemical Reviews, 2017, 117(9): 6225−6331.

[69] LIU K H, ZHONG H X, LI S J, et al. Advanced catalysts for sustainable hydrogen generation and storage via hydrogen evolution and carbon dioxide/nitrogen reduction reactions[J]. Progress in Materials Science, 2018, 92: 64−111.

[70] WU C, WANG X Y, PEI W L, et al. Tailoring the shape and size of wet-chemical synthesized FePt nanoparticles by controlling nucleation and growth with a high magnetic field[J]. Nanoscale, 2019, 11(32): 15023−15028.

[71] WANG X Y, LIU C H, WU C, et al. Magnetic field assisted synthesis of Co_2P hollow nanoparticles with controllable shell thickness for hydrogen evolution reaction[J]. Electrochimica Acta, 2020, 330: 135191.

[72] LIN Y, LIU M, PAN Y, et al. Porous Co-Mo phosphide nanotubes: An efficient electrocatalyst for hydrogen evolution[J]. Journal of Materials Science, 2017, 52(17): 10406−10417.

[73] TANG C, ASIRI A M, LUO Y, et al. Electrodeposited Ni-P alloy nanoparticle films for efficiently catalyzing hydrogen- and oxygen-evolution reactions[J]. ChemNanoMat, 2015, 1(8): 558−561.

[74] CHANG J F, LI K, WU Z J, et al. Sulfur-doped nickel phosphide nanoplates arrays: A monolithic electrocatalyst for efficient hydrogen evolution reactions[J]. ACS Applied Materials & Interfaces, 2018, 10(31): 26303−26311.

[75] PI M Y, WANG X D, ZHANG D K, et al. A 3D porous WP_2 nanosheets@carbon cloth flexible electrode for efficient electrocatalytic hydrogen evolution[J]. Frontiers of Chemical Science and Engineering, 2018, 12(3): 425−432.

[76] ZHANG X Y, WU Z Z, WANG D Z. Oxygen-incorporated defect-rich MoP for highly efficient hydrogen production in both acidic and alkaline media[J]. Electrochimica Acta, 2018, 281: 540−548.

[77] GAO W K, CHI J Q, WANG Z B, et al. Optimized bimetallic nickel-iron phosphides with rich defects as enhanced electrocatalysts for oxygen evolution reaction[J]. Journal of Colloid and Interface Science, 2019, 537: 11−19.

[78] LIN J H, YAN Y T, XU T X, et al. Rich P vacancies modulate Ni_2P/Cu_3P interfaced nanosheets for electrocatalytic alkaline water splitting[J]. Journal of Colloid and Interface Science, 2020, 564: 37−42.

[79] KWONG W L, GRACIA-ESPINO E, LEE C C, et al. Cationic vacancy defects in iron phosphide: A promising route toward efficient and stable hydrogen evolution by electrochemical water splitting[J]. Chem Sus Chem, 2017, 10(22): 4544−4551.

[80] CHENG W R, ZHANG H, ZHAO X, et al. A metal-vacancy-solid-solution NiAlP nanowall array bifunctional electrocatalyst for exceptional all-pH overall water splitting[J]. Journal of Materials Chemistry A, 2018, 6(20): 9420−9427.

[81] DAUN J J, CHEN S, ORTÍZ-LEDÓN C A, et al. Phosphorus vacancies that boost electrocatalytic hydrogen evolution by two orders of magnitude[J]. Angewandte Chemie International Edition, 2020, 59(21): 8181−8186.

[82] WANG Z K, WANG S Y, MAL X, et al. Water-induced formation of Ni_2P-$Ni_{12}P_5$ interfaces with superior electrocatalytic activity toward hydrogen evolution reaction[J]. Small, 2021, 17(6): 2006770.

[83] LIN J H, YAN Y T, LIU T, et al. Optimize the electrocatalytic performances of NiCoP for water splitting by the synergic effect of S dopant and P vacancy[J]. International Journal of Hydrogen Energy, 2020, 45(32): 16161−16168.

[84] RAN Z, SHU C, HOU Z, et al. Modulating electronic structure of honeycomb-like Ni_2P/$Ni_{12}P_5$ heterostructure with phosphorus vacancies for highly efficient lithium-oxygen batteries[J]. Chemical Engineering Journal, 2021, 413: 127404.

[85] WANG Y Q, ZHANG J T. Structural engineering of transition metal-based nanostructured electrocatalysts for efficient water splitting[J]. Frontiers of Chemical Science and Engineering, 2018, 12(4): 838−854.

[86] WANG Y, KONG B, ZHAO D Y, et al. Strategies for developing transition metal phosphides as heterogeneous electrocatalysts for water splitting[J]. Nano Today, 2017, 15: 26−55.

[87] HUANG X, LIU Z, MILLET M M, et al. In situ atomic-scale observation of surface-tension-induced structural transformation of Ag-NiP_x core-shell nanocrystals[J]. ACS Nano, 2018, 12(7): 7197−7205.

[88] WANG X Q, CHEN Y F, YU B, et al. Hierarchically porous W-doped CoP nanoflake arrays as highly efficient and stable electrocatalyst for pH-universal hydrogen evolution[J]. Small, 2019, 15(37): 1902613.

[89] 孙学良. 富磷型贵金属磷化物的绿色制备及电催化[J]. 物理化学学报, 2020, 37: 2011077.
SUN Xue-liang. Green synthesis and electrocatalysis of P-rich noble metal phosphides[J]. Journal of the Physical Chemistry, 2020, 37: 2011077.

[90] WANG J, LI X Z, WEI B, et al. Activating basal planes of $NiPS_3$ for hydrogen evolution by nonmetal heteroatom doping[J]. Advanced Functional Materials, 2020, 30(12): 1908708.

[91] LI Y J, WANG M, LIU S, et al. Preparation and properties of transition metal nitrides caged in N-doped hollow porous carbon sphere for oxygen reduction reaction[J]. Transactions of Nonferrous Metals Society of China, 2021, 31(5): 1427−1438.

[92] XU K, DING H, ZHANG M X, et al. Regulating water-reduction kinetics in cobalt phosphide for enhancing HER catalytic activity in alkaline solution[J]. Advanced Materials, 2017, 29(28): 1606980.

[93] FANG Z, PENG L, QIAN Y, et al. Dual tuning of Ni-Co-A (A=P, Se, O) nanosheets by anion substitution and holey engineering for efficient hydrogen evolution[J]. Journal of the American Chemical Society, 2018, 140(15): 5241−5247.

[94] PAN Y, SUN K A, LIN Y, et al. Electronic structure and d-band center control engineering over M-doped CoP (M= Ni, Mn, Fe) hollow polyhedron frames for boosting hydrogen production[J]. Nano Energy, 2019, 56: 411−419.

[95] LIU T T, MA X, LIU D N, et al. Mn doping of CoP nanosheets array: An efficient electrocatalyst for hydrogen evolution reaction with enhanced activity at all pH values[J]. ACS Catalysis, 2017, 7(1): 98−102.

[96] ZHANG G, WANG G C, LIU Y, et al. Highly active and stable catalysts of phytic acid-derivative transition metal phosphides for full water splitting[J]. Journal of the American Chemical Society, 2016, 138(44): 14686−14693.

[97] ZHANG J T, SUI R, XUE Y R, et al. Direct synthesis of parallel doped N-MoP/N-CNT as highly active hydrogen evolution reaction catalyst[J]. Science China Materials, 2019, 62(5): 690−698.

[98] XU K, SUN Y, SUN Y, et al. Yin-Yang harmony: Metal and nonmetal dual-doping boosts electrocatalytic activity for alkaline hydrogen evolution[J]. ACS Energy Letters, 2018, 3(11): 2750−2756.

[99] TIAN G Q, WEI S R, GUO Z T, et al. Hierarchical $NiMoP_2$-Ni_2P with amorphous interface as superior bifunctional electrocatalysts for overall water splitting[J]. Journal of Materials Science & Technology, 2021, 77: 108−116.

[100] WU C, CAI J J, ZHU Y, et al. Hybrid reduced graphene oxide nanosheet supported Mn-Ni-Co ternary oxides for aqueous asymmetric supercapacitors[J]. ACS Applied Materials & Interfaces, 2017, 9(22): 19114−19123.

[101] TIAN J Q, LIU Q, CHENG N Y, et al. Self-supported Cu_3P nanowire arrays as an integrated high-performance three-dimensional cathode for generating hydrogen from water[J]. Angewandte Chemie International Edition, 2014, 53(36): 9577−9581.

[102] TANG C, ZHANG R, LU W B, et al. Fe-doped CoP nanoarray: A monolithic multifunctional catalyst for highly efficient hydrogen generation[J]. Advanced Materials, 2017, 29(2): 1602441.

[103] LIANG Y H, LIU Q, ASIRI A M, et al. Self-supported FeP nanorod arrays: A cost-effective 3D hydrogen evolution

cathode with high catalytic activity[J]. ACS Catalysis, 2014, 4(11): 4065−4069.

[104] TIAN J, LIU Q, LIANG Y, et al. FeP nanoparticles film grown on carbon cloth: An ultrahighly active 3D hydrogen evolution cathode in both acidic and neutral solutions[J]. ACS Applied Materials & Interfaces, 2014, 6(23): 20579−20584.

[105] TONG M M, WANG L, YU P, et al. 3D Network nanostructured NiCoP nanosheets supported on N-doped carbon coated Ni foam as a highly active bifunctional electrocatalyst for hydrogen and oxygen evolution reactions[J]. Frontiers of Chemical Science and Engineering, 2018, 12(3): 417−424.

[106] WU Z X, WANG J, ZHU J, et al. Highly efficient and stable MoP-RGO nanoparticles as electrocatalysts for hydrogen evolution[J]. Electrochimica Acta, 2017, 232: 254−261.

[107] RIYAJUDDIN S, AZMI K, PAHUJA M, et al. Super-hydrophilic hierarchical Ni-foam-graphene-carbon nanotubes-Ni_2P-CuP_2 nano-architecture as efficient electrocatalyst for overall water splitting[J]. ACS Nano, 2021, 15(3): 5586−5599.

Recent progress of transition metal phosphides in hydrogen evolution reaction of electrolyzed water

WANG Zhong[1], LIU Jia-qi[1], LIU Chen[1], YUAN Shuang[1, 3, 4], WANG Qiang[2]

(1. School of Metallurgy, Northeastern University, Shenyang 110819, China;
2. Key Laboratory of Material Electromagnetic Process Research Ministry of Education, Northeastern University, Shenyang 110819, China;
3. Institute for Frontier Technologies of Low-Carbon Steelmaking, Northeastern University, Shenyang 110819, China
4. Liaoning Province Engineering Research Center for Technologies of Low-Carbon Steelmaking, Northeastern University, Shenyang 110819, China)

Abstract: In recent years, with the development of society, the consumption of traditional fossil energy has increased dramatically, and the environmental problems have become increasingly serious. Electrochemical water decomposition is a practical strategy for converting electric energy into hydrogen fuel. Therefore, in order to achieve large-scale hydrogen production, it is very important to develop low-cost, resource rich, efficient and stable electrocatalysts. Transition metal phosphides are widely used in the field of electrocatalytic dilute hydrogen because of their low price, good conductivity and chemical stability. In this paper, the preparation methods of transition metal phosphides for electrocatalytic hydrogen evolution were summarized, and the improvement of hydrogen evolution performance of electrolyzed water from three aspects of morphology design, interface control and material composite were summarized in detail. The future development trend, opportunities and challenges are also prospected.

Key words: transition metal phosphide; hydrogen evolution reaction; morphology design; interface control; material composite

Foundation item: Project(21701022) supported by the National Natural Science Foundation of China; Project (2018QNRC001) supported by the Young Elite Scientists Sponsorship Program by CAST; Project(XLYC1807214) supported by the Liaoning Revitalization Talents Program, China; Project(N2124007-1) supported by the Fundamental Research Funds for the Central Universities, China

Received date: 2021-05-06; **Accepted date:** 2021-08-19

Corresponding author: YUAN Shuang; Tel: +86-24-83681171; E-mail: yuans@smm.neu.edu.cn

(编辑　龙怀中)